Feasibility of Fluorodeoxyglucose Dual-Head Gamma Camera Coincidence Imaging in the Evaluation of Lung Cancer: Comparison with FDG PET

Mitsuaki Tatsumi, Kenji Yutani, Yoshiyuki Watanabe, Shinichiro Miyoshi, Noriyuki Tomiyama, Takeshi Johkoh, Hideo Kusuoka, Hironobu Nakamura and Tsunehiko Nishimura

Division of Tracer Kinetics, Department of Radiology, First Department of Surgery, Osaka University Medical School, Osaka, Japan

The purpose of this study was to elucidate the feasibility of fluorodeoxyglucose gamma camera coincidence imaging (FDG GCI) in the evaluation of lung cancer in comparison with FDG PET. **Methods:** Twenty-three patients with recently diagnosed lung cancer were examined with both FDG PET and FDG GCI on the same day. Pulmonary lesions were analyzed visually and semiquantitatively using the ratio of lesion-to-background counts (L/B ratio). The L/B ratio of FDG PET without attenuation correction (AC) was also calculated and compared. Nodal stations were only visually analyzed. **Results:** FDG GCI and FDG PET could detect 22 and 23, respectively, of 23 pulmonary lesions by visual analysis (95.7% versus 100%). The L/B ratio of FDG GCI was 4.26 ± 2.55, and significantly lower than that of FDG PET (9.29 ± 4.95; $P < 0.01$). The L/B ratio of FDG PET was significantly higher with AC than that without AC (9.29 ± 4.95 vs. 6.66 ± 4.65; $P < 0.01$). When the L/B ratio threshold was set at 5.0 for FDG PET and 2.7 for FDG GCI, their sensitivity was 87.0% and 73.9%, respectively. Of the 3 and 6 patients with false-negative results on semiquantitative analysis, the lesions in 3 patients on FDG PET and 4 patients on FDG GCI were less than or equal to 2.0 cm in greatest diameter, respectively. In the assessment of mediastinal involvement, FDG PET was 77.8% sensitive, 78.6% specific and 78.3% accurate, whereas FDG GCI was 77.8% sensitive, 92.9% specific and 87.0% accurate. In the hilar regions, FDG PET was 100% sensitive, 84.2% specific and 87.0% accurate, whereas FDG GCI was 75.0% sensitive, 89.5% specific and 87.0% accurate. **Conclusion:** In this study, FDG GCI yielded results comparable to FDG PET on visual analysis to detect pulmonary lesions and lymph node metastases. However, the lesion-to-background contrasts of pulmonary lesions and nodal involvement were lower in FDG GCI than in FDG PET. Comparison between the L/B ratio of FDG PET with and without AC indicated that, with AC, FDG GCI would be closer to FDG PET in the evaluation of lung cancer.

Key Words: fluorodeoxyglucose; gamma camera coincidence imaging; PET; lung cancer

J Nucl Med 1999; 40:566–573

Lung cancer is a leading cause of death in many countries, and its incidence around the world is increasing. Early detection and accurate staging of the disease often present a diagnostic challenge. CT, currently the most widely used imaging modality, has played an important role in the evaluation of lung cancer. Although CT provides significant anatomic and morphologic information, it has several limitations, including limited ability to distinguish between benign and malignant tumors, and thus, the definitive diagnosis is still established by bronchoscopic or percutaneous biopsy. A multi-institutional trial demonstrated that CT is only 52% sensitive and 69% specific in regard to staging (1). This is not surprising, because CT relies solely on node size. PET, on the other hand, provides metabolic images. PET with [18F]-fluorodeoxyglucose (FDG) allows detection of the increased glucose uptake characteristic of malignant cells (2,3). FDG PET has been reported to be of great use in the initial diagnosis (4–9) and the staging of lung cancer (10–16), but it is far less common than CT. Recently, a new gamma camera with a coincidence detection system has been developed and has begun to be used clinically. The purpose of this study was to elucidate the feasibility of FDG imaging with the new gamma camera (FDG gamma camera coincidence imaging [FDG GCI]) in lung cancer in comparison with FDG PET.

MATERIALS AND METHODS

Twenty-three patients (14 men, 9 women; mean age 59.0 y) with recently diagnosed lung cancer were included in this study (Table 1). Of these, 21 patients underwent surgery and had nodal stations sampled. The remaining 2 patients were treated with chemotherapy, because chest CT and FDG PET suggested multiple mediastinal metastases. Histopathologic confirmation was only obtained by examination of bronchoscopic biopsy specimens in these 2 patients; however, mediastinal involvement was also confirmed by follow-up with CT and FDG PET.

There were 16 patients with adenocarcinomas, 5 patients with squamous cell carcinomas, and 2 patients with metastases. The size of the tumors ranged from 1.0 to 5.0 cm (mean ± SD 3.0 ± 1.1

TABLE 1
Summary of Data for Pulmonary Lesions

Patient	Age	Sex	Histologic type	Size* (cm)	Location	SUV PET	L/B Ratio PET	L/B Ratio PET w/o AC	L/B Ratio GCI
1	46	F	ad	1.0	lt. S^6	0.58	3.18	1.90	N
2	38	M	ad	1.2	rt. S^2	1.56	2.75	2.23	1.42
3	66	F	ad	1.7	lt. S^{1+2}	1.96	6.43	4.31	2.56
4	64	F	ad	2.0	rt. S^{10}	2.26	2.15	1.85	2.19
5	70	M	ad	2.5	rt. S^3	3.74	11.58	7.26	4.71
6	58	F	ad	2.5	lt. S^6	4.41	15.11	7.27	4.30
7	48	M	ad	2.5	rt. S^3	3.49	6.48	4.47	3.16
8	31	M	ad	2.8	rt. S^6	3.31	6.16	5.73	3.63
9	71	M	ad	3.0	lt. S^6	4.84	10.94	6.28	2.71
10	50	F	ad	3.0	lt. S^{1+2}	3.07	10.17	5.73	4.66
11	60	M	ad	3.0	lt. S^8	2.50	11.45	8.21	2.83
12	66	F	ad	3.5	lt. S^6	4.55	11.93	6.56	6.27
13	68	M	ad	3.5	lt. S^6	5.94	9.29	6.13	5.86
14	77	F	ad	5.0	rt. S^{7-10}	5.46	7.40	3.49	2.37
15	69	F	ad	5.0	rt. S^1	10.80	26.53	15.01	10.60
16	72	F	ad	5.0	rt. S^2	3.67	7.97	4.88	2.76
17	75	M	sq	2.2	lt. S^{8-9}	4.69	6.70	5.16	2.96
18	62	M	sq	3.0	lt. S^6	6.03	10.28	3.23	4.91
19	63	M	sq	3.0	lt. S^6	2.68	6.56	3.99	1.47
20	40	M	sq	3.2	lt. S^6	5.87	8.86	15.00	8.77
21	50	M	sq	3.5	rt. S^6	8.06	10.24	21.18	9.38
22	50	M	mt	2.0	lt. S^5	4.28	12.33	8.82	5.44
23	64	M	mt	4.5	rt. S^5	3.11	9.12	4.39	3.91

*Size in terms of greatest diameter.

SUV = standardized uptake value; L/B = lesion-to-background counts; AC = attenuation correction; PET w/o AC = PET without AC; GCI = gamma camera coincidence imaging; ad = adenocarcinoma; lt = left; N = not visualized; rt = right; sq = squamous cell carcinoma; mt = metastatic lung cancer.

cm) in greatest diameter. Three patients had tumors less than 2.0 cm in greatest diameter (patients 1, 2 and 3). Mediastinal and hilar lymph node metastases were detected in 9 and 4 patients, respectively (Table 2). Only 1 patient had insulin-dependent diabetes (patient 3), and the serum glucose level just before FDG injection in the other patients was less than 120 mg/dL (patient 3: 306 mg/dL). Written informed consent was obtained from all the patients who participated in this study, and the study protocol was approved by the Ethics Committee of Osaka University.

FDG PET

FDG PET was performed with a PET scanner, the Headtome V (Shimadzu Co., Kyoto, Japan), which has 32 rings and simultaneously produces 63 slices 3.125-mm thick along a 20-cm longitudinal field. Intrinsic resolution was 3.7-mm full width at half maximum (FWHM) at the center, and the sensitivity of the device was 4.4 × 10^5 cpm/kBq. Two bed positions were obtained to include the whole lung and the adrenal gland. After at least 4 h of fasting, a transmission scan for attenuation correction (AC) was performed for 20 min (10 min per bed position). Skin markers placed just before the transmission scan were used to reposition the patient correctly for the emission scan. Emission images were acquired for 20 min (10 min per bed position), 1 h after intravenous administration of 370 MBq (10 mCi) FDG.

FDG Gamma Camera Coincidence Imaging

FDG GCI was performed with a dual-head gamma camera (VERTEX Plus/MCD; ADAC Laboratories, Milpitas, CA), equipped with a coincidence detection system for FDG. The axial field of view was 380 mm, and the slice thickness was approximately 3 mm. The intrinsic resolution was 4.8-mm FWHM at the center, and sensitivity was 1.6 × 10^5 cpm/kBq. Thirty-two projections were acquired for 50 s per view with a 128 × 128 matrix. Because of the count limitation of this device, data acquisition was begun when the counts per second of a single detector decreased to 1–1.5 million; this took approximately 3 h after FDG administration. No AC was used.

Chest CT

Chest CT scans were performed with a Highspeed Advantage (GE Medical Systems, Milwaukee, WI). Contiguous 5-mm thick sections were obtained in the superior mediastinum, 3-mm thick sections in the hilum and 7-mm thick in the remaining area. Nonionic contrast material (iohexol, Omnipaque 300 Syringe; Daiichi Pharmaceutical, Tokyo, Japan) was injected with a power injector at 1.5 mL/s just before scanning. CT was used only to localize the abnormal uptake seen on PET images, and, thus, the CT images were interpreted before the PET study in every patient.

Evaluation of Pulmonary Lesions

FDG PET and FDG GCI images were interpreted independently by two readers, who referred to the chest CT images. Pulmonary lesions were analyzed visually and semiquantitatively. In the visual analysis, any increased FDG uptake relative to the surrounding

TABLE 2
Comparison of FDG PET and FDG GCI Findings in Regard to Lymph Node Metastases

Patient	Mediastinum PET	Mediastinum GCI	Mediastinum Pathology	Hilum PET	Hilum GCI	Hilum Pathology
1	N	N	N	N	N	N
2	N	N	N	N	N	N
3	P	N	N	N	N	N
4	N	N	N	N	N	N
5	P	N	N	P	P	N
6	P	P	N	P	P	N
7	N	N	P	N	N	N
8	N	N	N	P	N	N
9	P	P	P	N	N	N
10	N	N	N	N	N	N
11	N	N	N	N	N	N
12	N	N	N	P	N	P
13	N	N	P	P	P	P
14	P	P	P	P	P	P
15	N	N	N	N	N	N
16	N	N	N	N	N	N
17	N	N	N	N	N	N
18	P	P	P	P	P	P
19	P	P	P	N	N	N
20	P	P	P	N	N	N
21	P	P	P	N	N	N
22	P	P	P	N	N	N
23	N	N	N	N	N	N

GCI = gamma camera coincidence imaging; N = negative findings; P = positive findings.

normal lung was considered positive for tumor. In the semiquantitative analysis, regions of interest (ROIs) were selected at the most intense area of FDG accumulation for pulmonary lesion and at the homologous contralateral normal lung for background. The ratio of the lesion-to-background counts (L/B ratio) was calculated. The standardized uptake value (SUV) was also calculated in the PET images, according to the following formula: PET count × calibration factor (MBq/kg)/injection dose (MBq)/body weight (kg) (17). Although SUV is used commonly to assess lesions, the L/B ratio was used to compare FDG PET and FDG GCI in this study. Both the L/B ratio and SUV are accurate methods of diagnosing pulmonary lesions (9,18), and it is better to compare both modalities by the same technique. To clarify the effect of AC, PET images without AC were also reconstructed and compared.

Evaluation of Lymph Node Metastases

Only visual analysis of nodal involvement was performed. Foci of FDG uptake greater than the activity of surrounding normal tissue were considered positive for nodal metastases. Semiquantitative analysis was not performed, because the small size of the nodal metastases resulted in underestimation due to the partial volume effect.

Statistical Analysis

The data are expressed as mean ± SD. The L/B ratios by FDG PET, FDG PET without AC and FDG GCI were compared by one-way repeated measures analysis of variance, followed by contrast test. Probability values of less than 0.05 were considered statistically significant.

RESULTS

Pulmonary Lesions

Table 1 summarizes the results of the FDG PET and FDG GCI studies for pulmonary lesions. Representative FDG PET, FDG PET without AC and FDG GCI images of pulmonary lesions are shown in Figure 1.

On the basis of visual inspection, FDG PET allowed detection of all 23 pulmonary lesions (100%). FDG PET without AC also allowed detection of all the pulmonary lesions (100%). FDG GCI failed to detect one of them (95.7%). The tumor not visualized on FDG GCI was a 1.0-cm adenocarcinoma located in S^6 of the left lung (patient 1; Fig. 2).

The L/B ratios of FDG PET, FDG PET without AC and FDG GCI are shown in Figure 3. The L/B ratio of FDG PET was 9.29 ± 4.95 (2.15–26.53), and the L/B ratio of FDG GCI was 4.26 ± 2.55 (1–10.60) and significantly lower ($P <$ 0.01). However, there was a significant positive correlation between the L/B ratio of FDG PET and of FDG GCI ($r =$ 0.712, $P < 0.001$; Fig. 4). When the L/B ratio threshold on FDG PET was set at 5.0, as reported previously (9), 20 of 23 patients had true-positive results, a sensitivity of 87.0%. The 3 patients had false-negative results and had two lesions less than 2.0 cm in greatest diameter (patients 1 and 2) and one equal to 2.0 cm in greatest diameter (patient 4) (Fig. 5A). As shown in Figure 4, the L/B ratio of 5.0 on FDG PET corresponded to the L/B ratio of 2.7 on FDG GCI in this study. If the L/B ratio of 2.7 were used for a threshold for FDG GCI, 17 of 23 lesions would be true-positive, with a sensitivity of 73.9%. Six patients had false-negative results; 3 lesions were less than 2.0 cm in greatest diameter (patient 1, 2 and 3), 1 was equal to 2.0 cm in greatest diameter (patient 4) and 2 were greater than 2.0 cm in greatest diameter (patients 14 and 19) (Fig. 5B). Of the 6 patients who had false-negative results on FDG GCI, 3 patients were identical to those of FDG PET (patients 1, 2 and 4). FDG PET could detect only 33.3% of the lesions less than 2.0 cm in greatest diameter, whereas FDG GCI could not detect any lesions on semiquantitative analysis. On the other hand, the sensitivity of FDG PET and FDG GCI for lesions equal to or greater than 2.0 cm in greatest diameter was 95.0% and 85.0%, respectively. No correlation was observed between tumor size and the L/B ratio on either FDG PET or FDG GCI (Fig. 5). The L/B ratio of FDG PET without AC was 6.66 ± 4.65 (1.85–21.18), which was significantly lower than that of FDG PET with AC ($P < 0.01$) and significantly higher than that of FDG GCI ($P < 0.01$). There was a positive
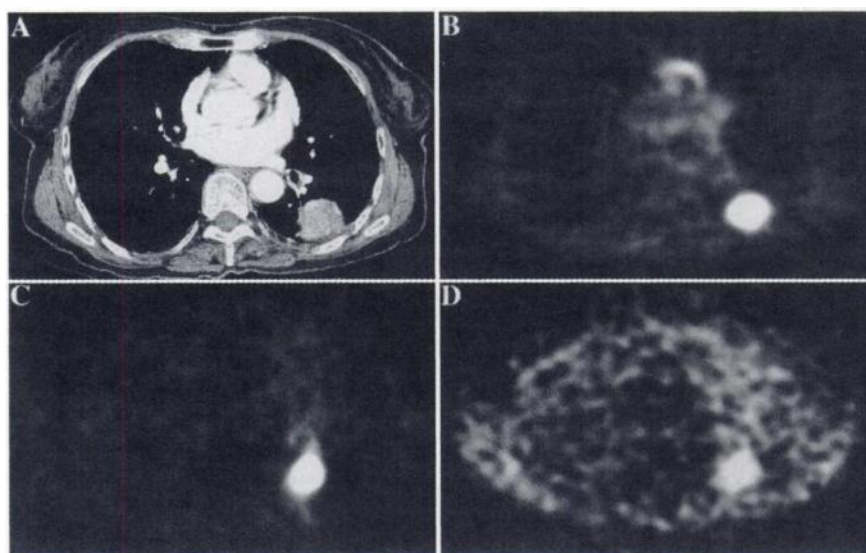

FIGURE 1. Patient 12, adenocarcinoma, 3.5 cm in greatest diameter. (A) Chest CT image shows tumor in left S^6. (B) FDG PET, (C) FDG PET without AC and (D) FDG GCI. All FDG images show pulmonary lesion. L/B ratio: (B) FDG PET, 11.93; (C) FDG PET without AC, 6.56; (D) FDG GCI, 6.27.
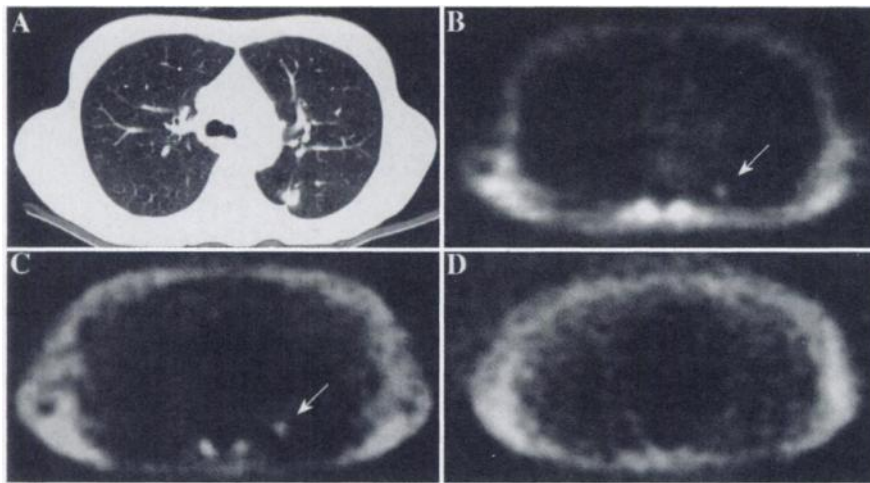
FIGURE 2. Patient 1, adenocarcinoma, 1.0 cm in greatest diameter. (A) Chest CT image shows tumor in left S^6. (B) FDG PET and (C) FDG PET without AC show uptake in tumor (arrow). (D) FDG GCI failed to detect lesion. L/B ratio: (B) FDG PET, 3.18; (C) FDG PET without AC, 1.90.

correlation between the L/B ratio of FDG PET without AC and the L/B ratio of FDG PET ($r = 0.577$, $P < 0.001$), as well as between the L/B ratio of FDG PET without AC and the L/B ratio of FDG GCI ($r = 0.869$, $P < 0.001$).

The SUV of the pulmonary lesions on FDG PET was 4.21 ± 2.22 (0.58–10.80). Significant positive correlations were observed between SUV and the L/B ratio of FDG PET ($r = 0.753$, $P < 0.01$), between SUV and FDG PET without AC ($r = 0.726$, $P < 0.01$) and between SUV and FDG GCI ($r = 0.848$, $P < 0.01$).

Lymph Node Metastases

The FDG PET and FDG GCI findings for lymph node metastases are summarized in Table 2. Representative FDG PET and FDG GCI images of mediastinal lymph node metastases are shown in Figure 6.

In 18 of 23 patients, FDG PET accurately predicted the mediastinal involvement. There were 3 patients with false-

positive results and 2 patients with false-negative results. Thus, the sensitivity, specificity, accuracy of FDG PET were 77.8%, 78.6% and 78.3%, respectively. All 3 false-positive findings were due to inflammatory nodes; 2 with slightly greater activity (patients 3 and 5) and the other with substantially greater activity (patient 6; Fig. 7), compared with surrounding normal mediastinum. In the 2 patients with false-negative results, the nodes were less than 1 cm in short-axis diameter on the chest CT (patients 7 and 13). FDG GCI correctly identified 7 of 9 patients with positive results and 13 of 14 patients with negative results for mediastinal involvement. The solitary false-positive node had substantially greater activity than that of surrounding normal tissue, which was also false-positive on PET (patient 6; Fig. 7). Two patients who had false-negative results were identical to those of PET (patients 7 and 13). The sensitivity, specificity and accuracy of FDG GCI were 77.8%, 92.9% and 87.0%, respectively.

In the hilar regions, FDG PET detected all 4 patients who had involvement. There were 3 patients with false-positive results: 1 with substantially greater activity (patient 6) and the other 2 with slightly greater activity (patients 5 and 8), compared with surrounding normal structures. The sensitivity, specificity and accuracy of FDG PET were 100%, 84.2% and 87.0%, respectively. FDG GCI correctly identified

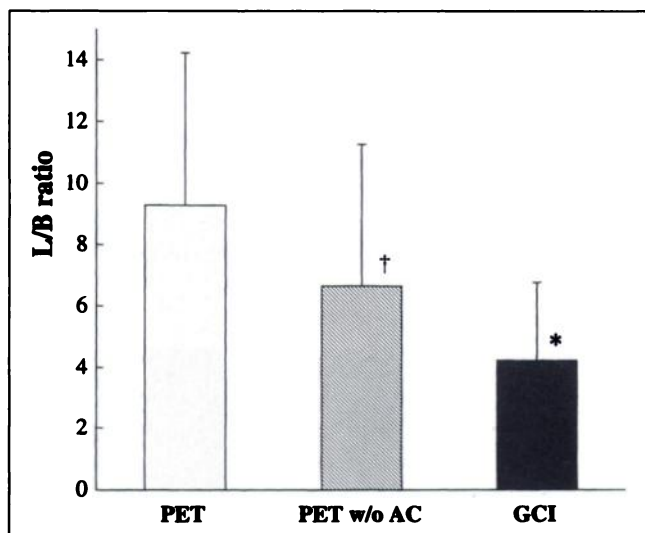**FIGURE 3.** Comparison of L/B ratios of FDG PET, FDG PET without AC and FDG GCI. L/B ratio of FDG GCI (4.26 ± 2.55) was significantly lower than obtained by FDG PET and FDG PET without AC (9.29 ± 4.95 and 6.66 ± 4.65, *$P < 0.01$, respectively). †$P < 0.01$ versus PET.
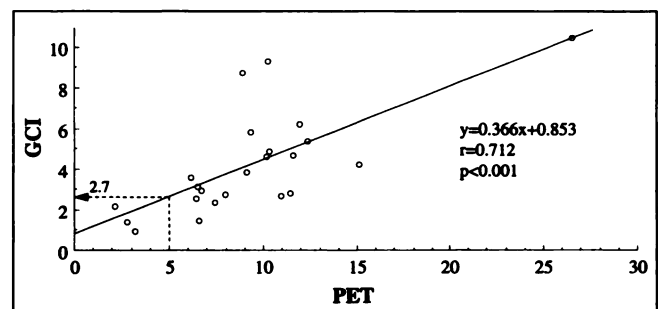

FIGURE 4. Relationship between L/B ratio of FDG PET and FDG GCI. Significant positive correlation was observed between L/B ratios obtained by FDG PET and FDG GCI. L/B ratio of 5.0 on FDG PET corresponded to L/B ratio of 2.7 on FDG GCI.

FIGURE 5. Relationship between tumor size and L/B ratios obtained by FDG PET (A) and FDG GCI (B). No correlation was observed between tumor size and L/B ratio by either FDG PET or FDG GCI. O = true-positive findings; ● = false-negative findings.
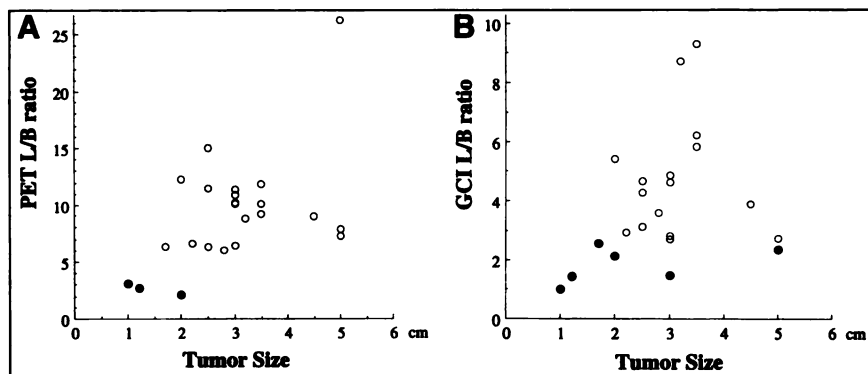
3 of 4 patients with positive results and 17 of 19 patients with negative results. The sensitivity, specificity and accuracy of FDG GCI were 75.0%, 89.5% and 87.0%, respectively. There were 2 patients with false-positive results: one with substantially greater activity (patient 6), and the other with slightly greater activity (patient 5), compared with normal hilum. There were also false-positive findings with PET. One lesion with false-negative results was less than 1.0 cm in short-axis diameter on chest CT (patient 12).

With regard to the assessment of the N2 status of the 21 patients with primary lung cancer, FDG PET was 75.0% sensitive, 76.9% specific and 76.2% accurate, whereas FDG GCI was 75.0% sensitive, 92.3% specific and 85.7% accurate.

DISCUSSION

FDG PET has been reported to be of great use for the initial diagnosis (4–9) and the staging (10–16) of lung cancer. Although FDG PET is known to be the optimal imaging modality for lung cancer at present, its availability as a clinical device is only limited. The requirement of a cyclotron to produce FDG is one of the reasons for this. However, an FDG-delivery system has already been achieved in some areas of the U.S. and other western countries (19). The situation seems to be gradually changing toward FDG imaging without an in-house cyclotron.

Another reason is the expensiveness of the PET camera. This has generated interest in using SPECT cameras as an alternative technique for FDG imaging (20–23). If FDG imaging with a SPECT camera can provide results similar to FDG PET, FDG imaging would become more widely used. The purpose of this study was to elucidate the feasibility of FDG GCI in lung cancer. Martin et al. (22) assessed the feasibility of FDG SPECT with 511-keV collimators in comparison with FDG PET in malignant tumors, including lung cancer. In their study, the sensitivity of the SPECT camera with 511-keV collimators was 4.8 cpm/MBq, and the spatial resolution was 17 mm-FWHM. The FDG SPECT detected 36 of 46 (78%) lesions identified by FDG PET (22). The gamma camera with coincidence detection system used in this study has a sensitivity of 1.6×10^5 cpm/kBq and a resolution of 4.8-mm FWHM. All but one (95.7%) of the pulmonary lesions yielded positive findings on visual analysis by FDG GCI, including a 1.2-cm adenocarcinoma. Although the study by Martin et al. (22) included several kinds of tumors, this study indicated that GCI is superior to SPECT with 511-keV collimators in the detection of lung cancer.

Lung cancer has been evaluated by using several radiopharmaceuticals such as ^{67}Ga and [201]Tl (24,25), as well as by using FDG. However, poor emission characteristics, availability problems and lack of specificity are significant disadvantages of these agents. Recently, ^{99m}Tc-methoxyiso-butylisonitrile (MIBI) has also been used for the evaluation of lung cancer (26–28). Labeling with ^{99m}Tc has several advantages over ^{67}Ga or ^{201}Tl, because ^{99m}Tc is readily available and has attractive nuclear properties for SPECT imaging. Nishiyama et al. (29) compared ^{99m}Tc-MIBI with ^{201}Tl in lung cancer and concluded that ^{99m}Tc-MIBI was not
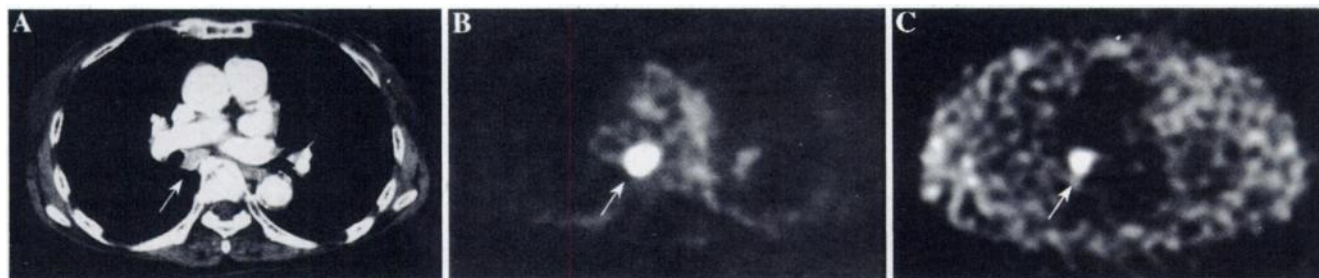

FIGURE 6. Patient 14, adenocarcinoma with mediastinal lymph node metastasis. (A) Chest CT image shows enlarged paraesophageal lymph node (arrow). (B) FDG PET and (C) FDG GCI show hot accumulation in node (arrow).
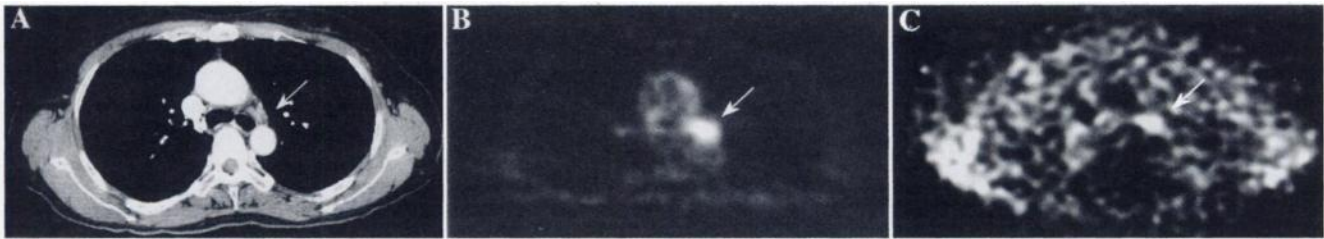
FIGURE 7. Patient 6, adenocarcinoma without lymph node metastasis, false-positive findings. (A) Chest CT image shows paratracheal lymph node (arrow) under 1.0 cm in short-axis diameter. Both FDG PET (B) and FDG GCI (C) show substantially greater activity in node compared with surrounding normal mediastinum (arrow).

superior to ^{201}Tl because of its lower L/B ratio and retention index. Although FDG shares some of the limitations of these radiopharmaceuticals, the relatively high L/B ratios in malignant lesions account for the high reported sensitivity and specificity of FDG imaging. In this study, not only FDG PET, but also FDG GCI showed high sensitivity in the detection of lung cancer (100% and 95.7%, respectively). However, the L/B ratio of FDG GCI was significantly lower than that of FDG PET (4.26 ± 2.55 versus 9.29 ± 4.95; $P <$ 0.01). Higashi et al. (30) compared FDG PET with ^{201}Tl in lung cancer patients. On the basis of visual analysis, in their study ^{201}Tl-SPECT yielded results similar to those of FDG PET in the detection of lung cancer ≥2 cm in diameter. The L/B ratios were 10.39 ± 6.63 for FDG PET and 3.01 ± 1.01 for ^{201}Tl-SPECT delayed scan, whereas in this study, the L/B ratios were 9.29 ± 4.95 for FDG PET and 4.26 ± 2.55 for FDG GCI. Assuming that there is a significant positive correlation between the L/B ratios obtained by FDG and ^{201}Tl in lung cancer, the L/B ratio of ^{201}Tl in this study would have been significantly lower than that of FDG GCI. The increased accumulation in the normal lung or adjacent myocardium may contribute to the lower L/B ratio of ^{201}Tl. The L/B ratio of FDG GCI and FDG PET would be higher than with other radiopharmaceuticals.

So far, no transmission scan sources for FDG GCI such as ^{137}Cs have been permitted in Japan. Therefore, the L/B ratio of FDG GCI in this study was calculated without using attenuation correction (AC). In cases of FDG PET in this study, the L/B ratio with AC was significantly higher than without AC (9.29 ± 4.95 versus 6.66 ± 4.65; $P <$ 0.01). Similarly, a higher L/B ratio of FDG GCI would be expected with AC. Coleman et al. (31) demonstrated in their phantom study that FDG GCI provided clearer images with AC than without AC, and that FDG GCI with AC allowed detection of a smaller sphere than without AC. AC on FDG GCI would yield lower lung activity as seen in the FDG PET with AC images. In a clinical situation, lesions are often evaluated only visually. The clearer FDG GCI images with AC would contribute significantly to the evaluation of lung cancer with visual inspection because of its higher lesion-to-background contrasts.

In the semiquantitative analysis for pulmonary lesions in this study, 3 FDG PET patients and 6 FDG GCI patients yielded false-negative findings. In all 3 patients with false-

negative results on FDG PET, the lesions were less than or equal to 2.0 cm in greatest diameter. There were also false-negative findings on FDG GCI. Although no statistical correlation was observed between tumor size and the L/B ratio either in FDG PET or FDG GCI in this study, the size of the lesion should affect scintigraphic detectability to some extent. Scintigraphic detectability would also depend on the contrast between lesion uptake and surrounding tissues (22). FDG GCI showed higher lung activity as a background, compared both with and without AC FDG PET in this study. With AC, FDG GCI would yield lower background activity. Another reason for the high background activity on FDG GCI is that FDG GCI had to be operated in the three-dimensional mode because of the limited detector efficiency. In PET studies, more scattered and random coincidences, which result in higher background activity, have been known to arise in the three-dimensional mode than in the two-dimensional mode (32,33). The same phenomenon must occur in FDG GCI in the three-dimensional mode. The three-dimensional mode also would yield limited spatial resolution with resultant worse lesion detectability. The two lesions of the 3 patients with false-negative results greater than 2.0 cm on FDG GCI were both located in the posterior and lower lung. Miyauchi et al. (34) reported that background ^{18}F activity is significantly increased in the posterior and lower lungs as compared with the upper and anterior lungs. This phenomenon may also provide a partial explanation for the false-negative findings on FDG GCI in this study.

The results of FDG PET in this study were slightly worse than reported previously in the detection of nodal involvement (10–16). FDG GCI, on the other hand, showed rather high specificity and accuracy, comparable to those of PET reported previously. Ironically, this phenomenon is due to the high sensitivity and high spatial resolution of the PET camera. FDG PET in this study yielded three mediastinal and three hilar false-positive findings. Of these, two mediastinal and two hilar nodes exhibited slightly greater activity than surrounding normal structures, and only one hilar node was detected on FDG GCI. The nodes were histopathologically demonstrated to be inflammatory or sarcoid nodes. All except one positive (true and false) finding on FDG GCI displayed substantially greater activity than the surrounding normal tissue on FDG PET. In retrospect, only nodes with

substantially greater activity than surrounding normal tissue should have been considered positive for nodal involvement on FDG PET. However, there was 1 patient with a true-positive hilar finding with slightly greater activity than the surrounding normal structures in this study. If FDG GCI with AC were used to assess nodal involvement, more patients with false-positive results would be expected. Further clinical trials are required to clarify the feasibility of FDG GCI in the assessment of metastatic nodes.

This study has certain limitations. First, it included only cases of malignant pulmonary lesions. Because the dual-head gamma camera with coincidence detection system has been developed recently, the study was focused on the feasibility of FDG imaging with the camera in the detection of lung cancer. This study shows that the sensitivity of FDG GCI for pulmonary lesions was comparable to that of FDG PET on visual analysis, and thus the next step is to clarify whether FDG GCI has the ability to distinguish between benign and malignant lung tumors. Second, this study included only three pulmonary lesions less than 2.0 cm in greatest diameter. Although both FDG PET and FDG GCI demonstrated high sensitivity for those lesions on visual analysis, both images showed rather low sensitivity on semiquantitative analysis. Further clinical studies are required to assess the feasibility of FDG GCI in small pulmonary lesions. Third, FDG GCI had to be begun 3 h after the injection of 370 MBq (10 mCi) FDG, because of the count limitation of this device. Tumor concentrations of FDG have been reported to increase until several hours after injection (35), whereas ^{18}F has a short half-life. The two modalities should be compared under the same conditions; however, FDG GCI yielded results similar to FDG PET on visual analysis in this study. Moreover, the protocol of this study enabled the patients to undergo FDG PET and FDG GCI on the same day, without an additional radiation dose. Another study is essential to determine the optimum scanning protocol for FDG GCI in the evaluation of lung cancer.

CONCLUSION

FDG GCI yielded results comparable to FDG PET on visual analysis to detect pulmonary lesions and lymph node metastases in this study. However, the lesion-to-background contrasts of pulmonary lesions and nodal involvement were lower in FDG GCI than in FDG PET. Comparison between the L/B ratio of FDG PET with and without AC indicated that, with AC, FDG GCI would be closer to FDG PET in the evaluation of lung cancer.

REFERENCES

1. Webb WR, Gatsonis C, Zerhouni EA, et al. CT and MR imaging in non-small cell bronchogenic carcinoma: report of the Radiologic Diagnostic Oncology Group. *Radiology.* 1991;178:705–713.
2. Som P, Atkins HL, Bandoypadhyay D, et al. A fluorinated glucose analog, 2-fluoro-2-deoxy-D glucose (F-18): nontoxic tracer for rapid tumor detection. *J Nucl Med.* 1980;21:670–675.
3. Wahl RL, Hutchins G, Buchsbaum D, Liebert M, Grossman HB, Fisher S. ^{18}F-2-deoxy-2-fluoro-D-glucose (FDG) uptake in human tumor xenografts: feasibility studies for cancer imaging with PET. *Cancer.* 1991;67:1544–1550.
4. Nolop KB, Rhodes CG, Brudin LH, et al. Glucose utilization in vivo by human pulmonary neoplasms. *Cancer.* 1987;60:2682–2689.
5. Kubota K, Matsuzawa T, Fujiwara T, et al. Differential diagnosis of lung tumor with positron emission tomography: a prospective study. *J Nucl Med.* 1990;31:1927–1932.
6. Gupta NC, Frank AR, Dewan NA, et al. Solitary pulmonary nodules: detection of malignancy with PET with 2-[F-18]-fluoro-2-deoxy-D-glucose. *Radiology.* 1992;184:441–444.
7. Patz EF Jr, Lowe VJ, Hoffman JM, et al. Focal pulmonary abnormalities: evaluation with F-18 fluorodeoxyglucose PET scanning. *Radiology.* 1993;188:487–490.
8. Dewan NA, Gupta NC, Redepenning LS, Phalen JJ, Frick MP. Diagnostic efficacy of PET-FDG imaging in solitary pulmonary nodules. Potential role in evaluation and management. *Chest.* 1993;104:997–1002.
9. Knight SB, Delbeke D, Stewart JR, Sandler MP. Evaluation of pulmonary lesions with FDG-PET. Comparison of findings in patients with and without a history of prior malignancy. *Chest.* 1996;109:982–988.
10. Wahl RL, Quint LE, Greenough RL, Meyer CR, White RI, Orringer MB. Staging of mediastinal non-small cell lung cancer with FDG PET, CT, and fusion images: preliminary prospective evaluation. *Radiology.* 1994;191:371–377.
11. Chin R Jr, Ward R, Keyes JW, et al. Mediastinal staging of non-small-cell lung cancer with positron emission tomography. *Am J Respir Crit Care Med.* 1995;152:2090–2096.
12. Patz EF Jr, Lowe VJ, Goodman PC, Herndon J. Thoracic nodal staging with PET imaging with ^{18}FDG in patients with bronchogenic carcinoma. *Chest.* 1995;108:1617–1621.
13. Sazon DA, Santiago SM, Soo Hoo GW, et al. Fluorodeoxyglucose-positron emission tomography in the detection and staging of lung cancer. *Am J Respir Crit Care Med.* 1996;153:417–421.
14. Sasaki M, Ichiya Y, Kuwabara Y, et al. The usefulness of FDG positron emission tomography for the detection of mediastinal lymph node metastases in patients with non-small cell lung cancer: a comparative study with X-ray computed tomography. *Eur J Nucl Med.* 1996;23:741–747.
15. Guhlmann A, Storck M, Kotzerke J, et al. Lymph node staging in non-small cell lung cancer: evaluation by [^{18}F]FDG positron emission tomography (PET). *Thorax.* 1997;52:438–441.
16. Steinert HC, Hauser M, Allemann F, et al. Non-small cell lung cancer: nodal staging with FDG PET versus CT with correlative lymph node mapping and sampling. *Radiology.* 1997;202:441–446.
17. Zasadny KR, Wahl RL. Standardized uptake values of normal tissues at PET with 2-[fluorine-18]-fluoro-2-deoxy-D-glucose: variations with body weight and a method for correction. *Radiology.* 1993;189:847–850.
18. Lowe VJ, Hoffman JM, Delong DM, Patz EF Jr, Coleman RE. Semiquantitative and visual analysis of FDG-PET images in pulmonary abnormalities. *J Nucl Med.* 1994;35:1771–1776.
19. Slosman DO, Spiliopoulos A, Couson F, et al. Satellite PET and lung cancer: a prospective study in surgical patients. *Nucl Med Commun.* 1993;14:955–961.
20. Van Lingen A, Huijgens PC, Visser FC, et al. Performance characteristics of a 511-keV collimator for imaging positron emitters with a standard gamma camera. *Eur J Nucl Med.* 1992;19:315–321.
21. Drane WE, Abbott FD, Nicole MW, Mastin ST, Kuperus JH. Technology for FDG SPECT with a relatively inexpensive gamma camera. *Radiology.* 1994;191:461–465.
22. Martin WH, Delbeke D, Patton JA, Sandler MP. Detection of malignancies with SPECT versus PET, with 2-[fluorine-18]fluoro-2-deoxy-D-glucose. *Radiology.* 1996; 198:225–231.
23. Holle LH, Trampert L, Lung Kurt S, et al. Investigations of breast tumors with fluorine-18-fluorodeoxyglucose and SPECT. *J Nucl Med.* 1996;37:615–622.
24. Matsuno S, Tanabe M, Kawasaki Y, et al. Effectiveness of planar image and single photon emission tomography of thallium-201 compared with gallium-67 in patients with primary lung cancer. *Eur J Nucl Med.* 1992;19:86–95.
25. Abdel Dayem HM, Scott A, Macapinlac H, Larson S. Tracer imaging in lung cancer. *Eur J Nucl Med.* 1994;21:57–81.
26. Hassan IM, Sahweil A, Constantinides C, et al. Uptake and kinetics of technetium-99m-hexakis 2-methoxy isobutyl isonitrile in benign and malignant lesions in the lungs. *Clin Nucl Med.* 1989;14:333–340.
27. Actolun C, Bayhan H, Kir M. Clinical experience with technetium-99m-MIBI imaging in patients with malignant tumors: preliminary results and comparison with thallium-201. *Clin Nucl Med.* 1992;17:171–176.

28. Kao CH, Wang SJ, Lin WY, Hsu CY, Liao SQ, Yeh SH. Differentiation of single solid lesions in the lungs by means of single photon emission tomography with technetium-99m-methoxyisobutylisonitrile. *Eur J Nucl Med.* 1993;20:249–254.

29. Nishiyama Y, Kawasaki Y, Yamamoto Y, et al. Technetium-99m-MIBI and thallium-201 scintigraphy of primary lung cancer. *J Nucl Med.* 1997;38:1358–1361.

30. Higashi K, Nishikawa T, Seki H, et al. Comparison of fluorine-18-FDG PET and thallium-201 SPECT in evaluation of lung cancer. *J Nucl Med.* 1998;39:9–15.

31. Coleman RE, Laymon CE, Turkington TG. Positron imaging of pulmonary nodules: phantom study [abstract]. *J Nucl Med.* 1998; 39(suppl):108p.

32. Budinger TF, Brennan KM, Moses WW, Derenzo SE. Advances in positron tomography for oncology. *Nucl Med Biol.* 1996; 23:659–667.

33. Cherry SR, Dahlbom M, Hoffman EJ. 3D PET using a conventional multislice tomograph without septa. *J Comput Assist Tomogr.* 1991;15:655–668.

34. Miyauchi T, Wahl RL. Regional 2-[^{18}F]fluoro-2-deoxy-D-glucose uptake varies in normal lung. *Eur J Nucl Med.* 1996;23:517–523.

35. Hamberg LM, Hunter GJ, Alpert NM, Choi NC, Babich JW, Fischman AJ. The dose uptake ratio as an index of glucose metabolism: useful parameter or oversimplification? *J Nucl Med.* 1994;35:1308–1312.